List of Figures

Regenerative chatter reduction by active damping control

A. Ganguli *, A. Deraemaeker, A. Preumont

Active Structures Lab, Université Libre de Bruxelles,

Av. F. D. Roosevelt, CP 165/42, Brussels 1050, Belgium.

Tel:+32 − 2 − 6502687, Fax:+32 − 2 − 6504660

*Corresponding Author e-mail: **ganguli@ecs.umass.edu**

Abstract

The objective of this paper is to demonstrate the effect of active damping on regenerative chatter instability for a turning operation. Two approaches are used for this purpose. In the first approach, the traditional stability analysis technique in [1] and other works is adopted and a correlation between the chip shape (which is dependent on the spindle speed) and the system damping is presented. It is shown that different spindle speeds cause changes in the system damping, resulting in different levels of stability limits at different spindle speeds. A second approach involves plotting of the root locus of the system poles with increasing axial width of cut. This study presents a different perspective to the problem. It is shown that the low and high stability regions of the stability lobe diagram are due to different relative positions of the poles and zeros of the system. Active damping is proposed as a strategy to enhance the stability limits of the system. The effect of active damping is

studied by the two approaches, mentioned above, both showing that active damping can successfully enhance the stability limits,particularly in the low stability regions.

Keywords: Regenerative Chatter, Stability lobe, Active Damping

1 Introduction

Machine tool chatter is a vibrational instability of the metal cutting process and is a popular topic for academic and industrial research. Although there are many mechanisms of chatter instability, as mentioned in Budak *et al.* [2], instability due to regeneration of surface waviness, demonstrated by Tobias *et al.* [3] and Tlusty [4], is by far the most common cause of chatter. Fig. (1) shows the regeneration process in an orthogonal cutting operation, where the tool is cutting a flexible cylindrical surface. While machining, due to vibrations, a wavy surface is left behind on the workpiece and after one full rotation the tool faces the waves left during the previous pass. This is the process of regeneration. Regenerative chatter was proposed as a closed loop interaction between the structural dynamics and the cutting process by Merrit [5]. Assuming the workpiece to be flexible only in the Y-direction, the uncut chip thickness $h(t)$ at any instant is given by,

$$h(t) = h_0 + y(t - T) - y \tag{1}$$

where h_0 is the constant feed of the tool, y and $y(t - T)$ are the displacements of the workpiece during the current and previous pass of the tool on the workpiece and $T = 60/N$ is the time of one revolution of the workpiece, with N as the rotational speed. Assuming that the cutting forces are proportional to the frontal area of the

chip, the cutting force in the Y direction is equal to

$$F_c(t) = K_f.a.[h_0 + y(t-T) - y] \tag{2}$$

a is the axial width of cut, measured in a direction perpendicular to the page and K_f is the cutting force constant. However, the cutting force and the chip thickness relationship is nonlinear and has been formulated through a power law in Taylor [6]. The nonlinearity in the cutting force and chip thickness relationship explains the subcritical Hopf Bifurcation phenomenon, as observed in Tobias *et al.* [7]. In a linear analysis, beyond a certain value of axial width of cut, the oscillations of the machine tool and workpiece system become unbounded. In reality, due to nonlinearity arising from the cutting process or the structure or both (Nayfeh *et al.* [8]) and due to the tool loosing contact with the workpiece (Tlusty *et al.* [9] and Sato *et al.* [10]), chatter manifests as high amplitude bounded oscillations called the limit cycle. The phenomenon is "subcritical" since the limit cycle continues to sustain itself at an axial width of cut lower than that predicted by the linear analysis. The nature of the phenomenon is therefore hysteric, as predicted in Nagy *et al.* [11], [12]. Further developments on the nonlinear dynamic analysis of regenerative chatter can be found in [13] and [14].

Damping from the cutting process and the machine tool structure are found to stabilize the machining process. Cutting process damping arises from the rubbing between the flank edge of the tool and the workpiece surface, leading to a dissipation of energy and stabilization of the cutting operation. This has been dealt with in Tobias *et al.* [3], Peters *et al.* [15], Tlusty [16] and Minis *et al.* [17]. Since the present work deals with the relationship between regenerative chatter instability and structural damping, the stabilizing effect of cutting process damping is ignored in the formulations. Enhancement of structural damping is possible by passive or active techniques and present study proposes the latter as a chatter suppression strategy. The authors

present a physical explanation of the role of structural damping in the phenomenon and the linear simplified cutting force model of Eq. 2 is adopted. Nonlinearities in the cutting process are beyond the scope of the current work. However, Pratt *et al.* [18], [19] [20] have shown experimental evidence of enhancement of axial depths of cut, due to application of active damping, even in the presence of nonlinearities in the system.

This paper is organized as follows. Section 2 discusses about the relationship between stability limits, spindle speed and structural damping using the traditional stability analysis technique. Section 3 uses the Root Locus technique to provide a pole-zero perspective to the ideas developed in Section 2. Section 4 discusses about the role of active damping in stabilization of regenerative chatter instability and its efficiency at various spindle speeds.

2 Discussions from traditional stability analysis perspective

Following the SDOF orthogonal model of cutting, the dynamic equation of motion can be written as,

$$m\ddot{y} + c\dot{y} + ky = K_f.a.[h_0 + y(t-T) - y] \tag{3}$$

where m, c and k are the mass, damping coeffcient and stiffness of the workpiece in the y direction. Eq. (3) is a time invariant Delay Differential equation. In Laplace domain $y(t-T) = y(s).e^{-sT}$. Defining the machine-tool transfer function between the applied force F_c and displacement y as $G(s)$ and substituting for $y(t-T)$, we have in Laplace domain,

$$\frac{h(s)}{h_0(s)} = \frac{1}{1 + K_f.a.G(s)(1 - e^{-sT})} \tag{4}$$

where

$$G(s) = \frac{y(s)}{F_c(s)} = \frac{1}{ms^2 + cs + k} \tag{5}$$

Therefore the characteristic equation of the closed loop system is

$$1 + K_{cut}.G(s)(1 - e^{-sT}) = 0 \tag{6}$$

where $K_{cut} = K_f.a$. From Eq. (6), K_{cut} can be derived as

$$K_{cut} = \frac{-1}{G(s)(1 - e^{-sT})} \tag{7}$$

Eq. (6) is not restricted to a single degree of freedom (SDOF) oscillator but can also be extended to single input single output (SISO) systems with multiple degrees of freedom, provided the appropriate expression for $G(s)$ is used. Following the traditional stability analysis technique as described in Altintas [1] and assuming that the system is at the stability limit and oscillating harmonically with chatter frequency ω_c, $s = j\omega_c$ is substituted in Eq. (6). Equating the real and imaginary parts to zero and with some mathematical manipulation, the following relationships are obtained.

$$K_{lim} = \frac{-1}{2\mathbf{Re}(G(j\omega_c))} \tag{8}$$

$$\omega_c T = 2p\pi - 2\tan^{-1}\left(\frac{\mathbf{Re}(G(j\omega_c))}{\mathbf{Im}(G(j\omega_c))}\right) = 2p\pi - \epsilon \tag{9}$$

where p $= 0, 1, ..$ and $\epsilon = 2\tan^{-1}\left(\frac{\mathbf{Re}(G(j\omega_c))}{\mathbf{Im}(G(j\omega_c))}\right)$. K_{lim} is inversely proportional to $\mathbf{Re}(G(s))$. Since stability limit is a physical quantity and is positive, Eq. (8) for a SDOF system is valid for values of ω_c, higher than the natural frequency of the machine tool structure, where $\mathbf{Re}(G(s))$ is less than zero. This proves that chatter frequencies should be higher than the natural frequency in a SDOF turning operation.

The plot of the stability limit and the chatter frequency, obtained by solving Eqs.

(8) and (9) for various spindle speeds is the traditional stability lobe diagram. An example of SDOF cutting operation with a rigid tool and flexible workpiece, modeled as a simply supported rectangular steel beam is solved with the traditional stability analysis technique. The corresponding tool point transfer function $G(s)$ in modal coordinates is given by Eq. (10)

$$G(s) = \sum_{i=1}^{n} \frac{\phi_i^2(x_a)}{\mu_i(s^2 + 2\xi_i\omega_i + \omega_i^2)} \tag{10}$$

where n is the number of modes considered, μ_i, ξ_i and ω_i are the modal mass, damping and frequency of the $i-$th mode and $\phi_i(x_a)$ is the mode shape calculated at the location of the tool, x_a on the beam. For demonstration purposes $n = 1$ is assumed in the calculations. The data for the calculation are : Young's modulus = 210 Mpa, length of beam $l = 1$ m, width $w = 0.01$ m, height $h = 0.02$ m, $x_a = \frac{l}{8}$ and density $\rho = 7800$ kg/m^3. The modal damping ratio ξ is assumed to be 1%. The beam is assumed to bend along the stiffer direction. Therefore, the natural frequency is about 47 Hz.

In figures 2 a), b) and c), the stability limits are presented and the various lobes are numbered according to the value of p, used in the calculation ($p = 0, 1, 2$ are used in the calculations). One can observe a repetition of the lobes, which arises from the trigonometric nature of Eq. (9). There is an overlap between successive lobes at certain spindle speeds. From the viewpoint of stability limit, the lower limit and the corresponding chatter frequency should be considered. Around the intersection points A and B, there is a jump in the chatter frequency and an abrupt change in the value of $\omega_c T$.

Physically $\omega_c T$ is the total angular displacement of the oscillating tool, vibrating with frequency ω_c during one period of revolution T. p is the number of complete waves traversed by the tool. Therefore, $\omega_c T$ is directly related to the phase difference between successive undulations on the workpiece surface, as shown in Fig. (3). The

implications of this phase difference on the stability of the system are now analyzed by considering four representative spindle speeds in Figs. (2) a), b) and c). The stability limits for 2700, 2840 and 8000 RPM are high and almost identical, but the chatter behavior, for these three cases is different. For 2700 and 8000 RPM, the phase $\omega_c T$ is close to an odd multiple of π. For 2840 RPM, where $\omega_c T = 2\pi$ and the chatter frequency ω_c and also the spindle speed frequency $1/T$ are nearly equal to the natural frequency of 47 Hz. For 3790 RPM, $\omega_c T = 3\pi/2 = 270$ degrees and the stability limit is the lowest. The correlation between the stability limit and phase difference between successive modulations of the chip thickness is being addressed now.

Writing Eq. (3) in frequency domain, we have

$$(-m\omega_c^2 + j\omega_c c + k)Y(j\omega_c) = K_{cut}[h_0 - (1 - e^{-j\omega_c T})Y(j\omega_c)] \tag{11}$$

Since the effect of the feed can be neglected in a linear analysis, the dynamic equation of motion can be written as,

$$[-m\omega_c^2 + j\omega_c(c + K_{cut}\frac{\sin\omega_c T}{\omega_c}) + (k + K_{cut} - K_{cut}\cos\omega_c T)]Y(j\omega_c) = 0 \tag{12}$$

It is observed in Eq. (12), that the damping and the stiffness of the system in the closed loop are frequency dependent, due to the term $\omega_c T$. Equating the real and the imaginary parts to zero, the values of K_{cut} and ω_c at the stability limit can be obtained. A direct relationship between the phase term $\omega_c T$, the damping coefficient and the stability limit is demonstrated by the following equation.

$$K_{lim} = -c\frac{\omega_c}{\sin\omega_c T} \tag{13}$$

Eq. (13) shows a proportional relationship between K_{lim} and the damping coefficient, which implies that higher axial widths of cut may be achieved without chatter by

enhancing structural damping. Considering the expression of stiffness in Eq. (12), it can be seen that there is a general stiffening of the structure due to regeneration process. For $\omega_c T$ approaching an odd multiple of π, K_{lim} tends to infinity. High stability limits are observable for 2700 and 8000 RPM in Fig. (2) a), for which the phase differences are nearly 180 and 540 degrees respectively. For the phase difference equal to 360 degrees or its even multiple, the stability limit is also infinity, from Eq. (13). This occurs for 2840 RPM (Refer to figures 2 a), b) and c)), where the spindle speed frequency, $1/T$, is close to the natural frequency. $\sin \omega_c T$ has a minimum value of -1, for $\omega_c T = \frac{3\pi}{2}$. Therefore a low value of K_{cut} is obtained from Eq. (13). This explains the low stability for 3790 RPM, for which the phase difference is equal to $\frac{3\pi}{2}$. A plot of $\omega_c / \sin \omega_c T$ is shown in Fig. (4) a). The discussion demonstrates the relationship between stability limits, structural damping and $\omega_c T$, i.e., the shape of the chip.

The vibrational behaviors for 2700, 2840 and 8000 RPM are qualitatively different even though the stability limits may be nearly equal to one another. In Region 1 in Fig. (4) b) (2840 RPM left end of lobe 1), the chip thickness is constant, due to the successive modulations of the chip thickness being in phase. Thus the structure will not be excited dynamically and ideally there is no possibility of chatter. For Regions 3 and 4 (2700 and 8000 RPM, right ends of lobes 2 and 1), the shape of the chip is highly deformed due to the successive undulations, being out of phase. This implies a strongly dynamic excitation force. However, the closed loop stiffness, depicted by the third term in Eq. (12), has a maximum value of $k + 2K_{cut}$. The qualitative differences in the behaviors in the two cases are observable in the time history plots of the force and displacement in Fig. (5). The absence of the regenerative effect for 2840 RPM causes the force to stabilize to a constant value. In the case of 2700 RPM, even though the force amplitude is high, the displacement level is almost identical to that of 2840 RPM. The existence of a higher closed loop stiffness explains this behavior. The section shows the qualitative difference between the instabilities in

the high stability regions of the stability lobe diagram and this knowledge is not very obvious.

3 Analysis by Root Locus Plots

The previous section shows a correlation between spindle speeds, the closed loop damping, the shape of the chip and the different levels of stability limits. The Root Locus method is used to investigate the correlation from a pole-zero perspective. Eq. (6) can be viewed as the characteristic equation of a classical closed loop system with unit feedback, as shown in Fig. (6). $G(s)(1-e^{-sT})$ is the open loop transfer function and K_{cut} is the feedback gain. The closed loop poles follow the corresponding root locus for increasing K_{cut} and the stability limit is reached when at least a couple of conjugate roots cross the imaginary axis. The transcendental part of the open loop transfer function, i.e., the delay term, gives rise to a system of time invariant Delay Differential Equation with infinite number of roots. It is approximated by Padé Approximation [21]. An explanation on the order of Padé Approximation to be assumed is presented in Ganguli *et al.* [22].

Eq. (6) generates two limit cases, depending on the value of K_{cut}.

- For $K_{cut} \to 0$, the roots are the poles of $G(s)(1 - e^{-sT})$ which are the poles of $G(s)$ and an infinite number of poles of $(1 - e^{-sT})$ at $s = -\infty \pm j(2n\pi/T)$, where $j = \sqrt{-1}$ and n is any integer.
- For cases where $K_{cut} \to \infty$, the roots are the zeros of $G(s)(1 - e^{-sT})$, which are the zeros of $G(s)$ and the infinite number of zeros of $(1 - e^{-sT})$ at $s = \pm j(2n\pi/T)$.

This is discussed by Olgac et al [23]. Fig. (7) shows the evolution of the poles for a SDOF system. For low values of K_{cut} the pole (denoted by a cross), closest to the imaginary axis, is a structural pole. The rest of the poles, due to the delay

term, ideally should be at infinite distance from the imaginary axis. But due to the approximation of the delay term and a non-zero initial value of K_{cut}, they are seen at finite but large distances from the imaginary axis. With increasing value of K_{cut}, all the roots approach the imaginary axis, implying a reduction in the damping of the closed loop system. Instability occurs when they cross the imaginary axis and with further increase in K_{cut}, the poles ultimately converge to the zeros at $s = \pm j(2n\pi/T)$, i.e. $s/2\pi = \pm j(n/T)$ in Hz units, where n as any integer. So the zeros of the system, due to the delay, are at harmonics of the spindle speed frequency. Traditional techniques of chatter analysis generally recognize that instability arises from the structural mode of the system. However, there is always a possibility, that the roots due to the delay may cross over to the right side of the imaginary axis before a structural pole does at certain spindle speeds. Thus different regions of the stability lobe diagram can be characterized, depending on whether the source of instability is a structural pole or a delay pole. Fig. (8) shows the stability lobe diagram and the chatter frequency diagrams for the SISO system example of the previous section. Different regions of the stability lobe and chatter frequency diagram are distinguished on the basis of the source of instability. The regions have been distinguished by following the locus of the closed loop poles for increasing values of K_{cut} and identifying which root is contributing to the instability. It is observed that certain portions of the high stability regions are due to instability of the delay pole. This is not very apparent from traditional stability analysis techniques. The Root Locus plots for the SISO example are examined for the representative spindle speeds of the previous section. The loci of the eigenvalues are plotted beyond the stability limit to show the direction of migration of the roots. The stable loci of the system is marked with a thin line and the unstable with a thicker line. It is seen in Fig. (9), that a reduction of the spindle speed, causes the poles and the zeros, due to the delay, to migrate towards the real axis. The proximity of the zero to the structural pole, determines the length of the locus to instability. A relatively distant location

of the zero, for 8000 RPM, in comparison to 3790 RPM, causes a longer locus of the structural pole to instability, resulting in higher stability in the former case. This is demonstrated in figures 9 a) and b). In Fig. (9) c), for 2840 RPM, the location of the zero in close proximity to the structural pole is causing a near pole-zero cancellation. The advancement of the pole towards instability is nullified and a very high value of K_{cut} is required to make the system unstable. The crossing of the pole to instability is very close to the natural frequency of the structure, indicating chatter frequency close to the natural frequency. For 2700 RPM, the zero migrates to a position below the structural pole. The close proximity of the zero to the pole also has a pole-zero cancellation effect and the structural pole does not contribute to instability. The instability arises from the delay pole and a very high value of K_{cut} is necessary for its migration from infinity to the imaginary axis. This explains a jump in the chatter frequency in Fig. (8) between 2700 and 2840 RPM. Thus very high chatter frequencies at certain spindle speeds can be attributed to the instability of the delay pole. The cases of 2700 and 8000 RPM are not qualitatively similar. For the former, the delay pole is contributing to instability and for the latter, the structural pole is the reason behind instability. The summary of this section is the following. The change in the spindle speed causes the poles and the zeros of the delay to move and this changes the behavior of the root locus and the instability characteristics. The high stability limits for certain spindle speeds (2700 and 2840 RPM, i.e., regions 1 and 4 in Fig. (4)) are explained by pole zero cancelation situations and instability due to the delay pole. The chatter frequency for turning is always higher than the natural frequency, since there is no crossing of the imaginary axis at frequencies lower than the natural frequency. High chatter frequencies, at certain spindle speeds, are associated with the delay pole instability. This fact is not very obvious from the traditional stability analysis technique. Low stability regions are due to instability of the structural pole that is located closer to the imaginary axis. Thus enhancement of structural damping (actively or passively) would shift the poles more to the left, which would necessitate

higher K_{cut} levels to destabilize the system. This observation confirms a similar idea from Eq. (13) from a pole-zero perspective and substantiates the original motivation of using active damping as a potential chatter reduction strategy. This is discussed in more detail in the next section.

4 Effect of active damping on chatter instability

The previous sections show that chatter can be stabilized by two methods: a) by choosing a spindle speed, where the phase between successive undulations is favorable b) by enhancing the structural damping. Eqs. (12) and (13) show that the two methods inherently affect the closed loop system damping and thus stabilize the system. Case a) is the easiest way to avoid chatter since a highly stable region exists between regions 1 and 4 in Fig. (4). The highly stable spindle speeds are regions where the closed loop damping is least "degraded" by the phase effect, as shown by Eq. (12). Online modification of spindle speed to this stable part of the stability lobe diagram was first proposed by Weck *et al.* [24]. The idea has been developed into an automated chatter recognition and spindle speed control system by sensing the acoustic signal from the cutting operation in Tlusty *et al.* [25], [26]. Soliman *et al.* [27] present a control system that ramps up the spindle speed until a stable machining situation is reached. Another technique of chatter stabilization is by spindle speed modulation, as proposed in [28], [29], [30] etc, where the spindle speed is varied periodically with a very low frequency.

Vibration control is another strategy to suppress chatter instability. Dohner et al [31] propose a pole placement strategy using a LQG controller and strain gage sensors and electrostrictive actuators for milling. Smart fluids such as electrorheological or magnetorheological fluids have been used for chatter suppression in Wang et al [32]

and Segalman et al [33]. Feedforward and adaptive control strategies are proposed in Nachtigal [34], [35] and Browning *et al.* [36] for chatter suppression in boring bars. Passive damping of chatter has been attempted through the "Lanchester" damper [37], impact dampers in [38] and tuned mass dampers in [39]. But the amount of damping achievable is limited and the performance of tuned mass dampers depends on the accurate tuning between the damper frequency and the structural modal frequency. In the present work the active damping strategy with collocated sensor and actuator configuration is proposed for regenerative chatter stabilization. A detailed study on active damping is presented in Preumont [40]. A collocated sensor and actuator configuration ensures an alternate pole-zero configuration of the structure in the complex plane and this ensures unconditional stability in the closed loop Miu [41], Preumont [40], provided the sensor and actuator dynamics are neglected. Even in the presence of sensor or actuator dynamics it can be shown that collocated active damping strategy fulfils the objective of enhancing modal damping of the structure (Zimmerman *et al.* [42]). Active damping by velocity feedback does not require a very accurate model of the structure and can be considered to be a broad band vibration control strategy. In the current work, a velocity feedback strategy is implemented similar to the works of Cowley et al [43] and Tewani et al [44]. Referring to Eqs. (12) and (13) for the SISO system, if the velocity at the tool contact point is fed back, then the enhanced stability limit is given by,

$$K_{lim} = -(c+g)\frac{\omega_c}{\sin \omega_c T} \tag{14}$$

where g is the feedback gain. The recent experimental studies on active damping of the machine tool for chatter reduction can be found in Pratt *et al.* [19] and Harms *et al.* [45]. Sims *et al.* [46], [47] apply active damping on the workpiece and Ganguli *et al.* [22] demonstrate the effect of active damping with a mechatronic chatter demonstrator. The stability lobes are plotted for two arbitrary values of feedback

gain in Fig. (10) a), for the SISO example. The damping of the structure in the two cases are 8.7% and 16%. A general rise in the stability limits is observed. It is also observed in 10) b) that active damping changes the frequency of chatter.

The factor of enhancement at various spindle speeds is now investigated. In Fig. (11) a), the ratio between the limiting cutting stiffness for two values of feedback gains and the corresponding value without any active damping is plotted. It is found that the enhancement of stability limit is the highest for the low stability regions, such as 3790 RPM. For spindle speeds of 2700, 2840 and 8000 RPM, with originally high stability limits, the factor of enhancement is not impressive. This can be explained again by referring to Fig. 11 b), which is a plot of $\omega_c / \sin \omega_c T$ for the different values of the active damping feedback gain. It is observed that for the high stability regions, there is a reduction in the absolute value of the quantity due to changes in the chatter frequency. This counteracts the effect of increased damping due to the feedback gain g in Eq. (14) and therefore affects the factor of increase in stability. In the case of spindle speeds, where the original stability limit is low (e.g. 3790 RPM), the change in the value of $\omega_c / \sin \omega_c T$ is negligible. The stability limit directly depends on the damping, coefficient. Therefore, the factor of increase in the low spindle speed cases is much higher in comparison to that in the high stability regions of the stability lobe diagram. This explains the non-uniform relative enhancements due to active damping for different spindle speeds.

The effect of active damping can also be demonstrated by Root Locus plots. The general effect of active damping is to shift the structural pole towards the left, due to enhanced damping. This implies that a higher cutting stiffness is necessary to make the system unstable, causing a rise in the stability limit. There is an increase in chatter frequency, due to the application of active damping, as are the cases for 8000 and 3790 RPM in Figs. (12) a) and b). The structural pole crosses the imaginary axis at higher frequencies than the chatter frequency without active damping and this explains the change in the chatter frequencies in Fig. (10) b). The relative

increase in the length of the closed loop locus of the structural pole, due to active damping, is higher in Fig. (12) b) than in a). In Fig. (12) c), the situation is close to a pole zero cancellation, as described in the previous section. It is interesting to see that due to active damping, the structural pole no longer becomes unstable. The delay pole triggers the instability. Thus active damping may change the nature of the instability. For 2700 RPM in Fig. (12) d), the delay pole becomes unstable with or without active damping, since the structural pole remains on the left side of the complex plane.

Certain observations can be made from the Root Locus plots. The structural poles are affected more by the application of active damping than the delay poles. For the low stability regions like 3790 RPM, active damping is relatively more effective in enhancing the stability limit than in the high stability regions. The delay poles, due to distant location from the imaginary axis do not undergo any appreciable change in damping. Therefore, the relative enhancement of stability is much higher in the low stability regions than the highly stable regions.

5 Conclusion

This paper presents a relationship between regenerative chatter instability and structural damping. The traditional stability analysis technique is reviewed and it is shown that the stability depends on two physical parameters: the structural damping in the system and the spindle speed that controls phase difference between successive modulations of the chip thickness, or in other words, the shape of the chip. The correlation between different shapes of the chip and the stability lobes is explained. Both of these parameters affect the closed loop system damping; enhancement of structural damping is shown to have a proportional effect on the stability limits, change of spindle speeds may cause a favorable or unfavorable phase difference between successive modulations which affect the closed loop damping and the stability limit. Normally for

a machine tool-workpiece system with a dominant natural frequency, regions where the spindle speed frequency is equal to the natural frequency are the highly stable machining areas. Root Locus plots are used to present a pole-zero perspective of the same idea. Highly stable regions of the stability lobe diagrams are found to be due to pole-zero cancelation between the structural pole and the delay zero or due to instability of the far located delay pole. Low stability regions are characterized by instability of a structural pole that is located close to the imaginary axis. This implies that enhancement of structural damping would result in higher stability limits in the low stability region areas.

Active damping with velocity feedback is adopted as the chatter control strategy in the present study. Active damping is found to affect both the structural damping and the phase difference between successive modulations of the chip thickness. The damping enhancement is predominant in the low stability regions of the stability lobe diagram, which results in a high rise in the stability limit. For high stability regions, the effect of active damping is counterbalanced by the change in the phase difference, resulting in a lesser improvement of the stability limit. The observation is substantiated by Root Locus plots which show that structural poles are affected more by active damping than delay poles. This implies that low stability limit regions would be enhanced more than the originally high stability regions due to active damping. The idea of utilizing active damping for regenerative chatter control has been recently implemented in the SMARTOOL project (www.smartool.org) funded by the European Commission.

6 Acknowledgement

The authors wish to thank the SMARTOOL Consortium and the European Commission for funding the project (Contract No. GIRD-CT-2001-00551). The authors also thank the Inter University Attraction Pole (IUAP S-06,AMS) programme between

Belgian Universities.

References

[1] Y. Altintas. *Manufacturing Automation*. Cambridge University Press, 2000.

[2] M. Wiercigroch and E. Budak. Sources of nonlinearities, chatter generation and suppression in metal cutting. *Philosophical Transactions of the Royal Society: Mathematical, Physical and Engineering Sciences*, 359:663–693, 2001.

[3] S.A. Tobias and W. Fishwick. Theory of regenerative machine tool chatter. *Engineering*, 205, 1958.

[4] J. Tlusty and M. Polacek. The stability of machine tools against self-excited vibrations in machining. *International Research in Production Engineering*, pages 465–474, 1963.

[5] H. E. Merrit. Theory of self-excited machine-tool chatter-contribution to machine tool chatter research-1. *ASME Journal of Engineering for Industry*, 87(4):447–454, 1965.

[6] F. W. Taylor. On the art of cutting metals. *Transactions of the ASME*, 28, 1907.

[7] S. A. Shi, H. M. Tobias. Theory of finite amplitude machine tool instability. *International Journal of Machine Tool Design and Research*, 24:45–69, 1984.

[8] A. H. Nayfeh, C. Chin, and J. Pratt. Perturbation methods in nonlinear dynamics - applications to machining dynamics. *ASME Journal of Manufacturing Science and Engineering*, 119:485–493, 1997.

[9] J. Tlusty and F. Ismail. Basic non-linearity in machining chatter. *Annals of the CIRP*, 30(1):299–304, 1981.

[10] O. Kondo, Y. Kawano and H. Sato. Behavior of self-excited chatter due to multiple regenerative effect. *ASME Journal of Engineering for Industry*, 103:324–329, 1981.

[11] T. Kalmar-Nagy, J. R. Pratt, M. A. Davies, and M. D. Kennedy. Experimental and analytical invetsigation of the subcritical instability in metal cutting. *Proceedings of DETC'99, 17th ASME Biennial Conference on Mechanical Vibration and noise, Nevada, USA*, 1999.

[12] F. C. Moon and T. Kalmar-Nagy. Nonlinear models for complex dynamics in cutting materials. *Philosophical Transactions of the Royal Society: Mathematical, Physical and Engineering Sciences*, 359:695–711, 2001.

[13] S. Gabor. Modelling nonlinear regenerative effects in metal cutting. *Philosophical Transactions of the Royal Society: Mathematical, Physical and Engineering Sciences*, 359:739–757, 2001.

[14] M. S. Fofana. Delay dynamical systems and applications to nonlinear machine tool chatter. *Chaos Solitons and Fractals*, 17:731–747, 2003.

[15] P. Peters, J. Vanherck and H. Van Brussel. The measurement of the dynamic cutting coefficient. *Annals of the CIRP*, 21, 1972.

[16] J. Tlusty. Analysis of the state of research in cutting dynamics. *Annals of the CIRP*, 27(2):583–589, 1978.

[17] I. Minis, E. Magrab, and I. Pandelidis. Improved methods for the prediction of chatter in turning, part 2: Determination of cutting process parameters. *ASME Journal of Engineering for Industry*, 112:21–27, 1990.

[18] J. Pratt. Vibration control for chatter suppression with application to boring bars. *Phd Thesis, Virginia Polytechnique Institute and State University*, 1997.

[19] J. Pratt and A. H. Nayfeh. Chatter control and stability analysis of a cantilever boring bar under regenerative cutting conditions. *Philosophical Transactions of*

the Royal Society: Mathematical, Physical and Engineering Sciences, 359:759–792, 2001.

[20] J. Pratt, M. A. Davies, C. J. Evans, and M. D. Kennedy. Dynamic interrogation of a basic cutting process. *Annals of the CIRP*, 48:39–43, 1999.

[21] J. Lam. Balanced realizations of pade approximants of e^{-sT} (all-pass case). *IEEE Transaction of Automatic Control*, 36(9):1096–1110, 1991.

[22] A. Ganguli, A. Deraemaeker, M. Horodinca, and A. Preumont. Active damping of chatter in machine tools - demonstration with a "hardware in the loop" simulator. *Journal of Systems and Control Engineering, Proceedings of the Institution of Mechanical Engineers*, 219(15):359–369, 2005.

[23] M. Olgac, N. Hosek. A new perspective and analysis for regenerative machine tool chatter. *International Journal of Machine Tools and Manufacture*, 38:783–798, 1998.

[24] M. Weck, E. Verhaag, and M. Gather. Adaptive control for face-milling operations with strategies for avoiding chatter vibrations and for automatic cut distribution. *Annals of the CIRP*, 24:405–409, 1975.

[25] T. Delio, J Tlusty, and S. Smith. Use of audio signals for chatter detection and control. *ASME Journal of Engineering for Industry*, 114:146–157, 1992.

[26] S. Smith and J. Tlusty. Stabilizing chatter by automatic spindle speed regulation. *Annals of the CIRP*, 41(1):433–436, 1992.

[27] E. Soliman and F. Ismail. A control system for chatter avoidance by ramping the spindle speed. *ASME Journal of Manufacturing Science and Engineering*, 120:674–683, 1998.

[28] T. Hoshi, N. Sakisaka, I. Moriyama, and M. Sato. Study of practical application of fluctuating speed cutting for regenerative chatter control. *Annals of the CIRP*, 25:175–179, 1977.

[29] B. J. Sexton, J. S. Stone. The stability of machining with continuosly varying spindle speed. *Annals of the CIRP*, 27:321–326, 1978.

[30] R. E. Lin, S. C. DeVor and S. G. Kapoor. The effects of variable speed cutting on vibration control in face milling. *ASME Journal of Engineering for Industry*, 112:1–11, 1990.

[31] J. L. Dohner, J. P. Lauffer, T. D. Hinnerichs, N. Shankar, M. Regelbrugge, C. Kwan, R. Xu, B. Winterbauer, and K. Bridger. Mitigation of chatter instabilities in milling by active structural control. *Journal of Sound and Vibration*, 269:197–211, 2004.

[32] M. Wang and R. Fei. Chatter suppression based on nonlinear vibration characteristic of electrorheological fluids. *International Journal of Machine Tools and Manufacture*, 39:1925–1934, 1999.

[33] D. Segalman and J. Redmond. Chatter suppression through variable impedance and smart fluids. *Proceedings of the SPIE*, 2721:353–363, 1996.

[34] C. Nachtigal. Design of a force feedback chatter control system. *ASME Journal of Dynamic Systems, Measurement and Control*, 94(1):5–10, 1972.

[35] C. Glaser, D. J. Nachtigal. Development of a hydraulic chambered, actively controlled boring bar. *ASME Journal of Engineering for Industry*, 101:362–368, 1979.

[36] D. R. Browning, I. Golioto, and N. B. Thompson. Active chatter control system for long-overhang boring bars. *Proceedings of the SPIE*, 3044:270–280, 1997.

[37] R. S. Hahn. Active dampers for machine tools. *Transactions of ASME*, 73:213–222, 1951.

[38] S. Ema and E. Marui. Suppression of chatter vibration of boring tools using impact dampers. *International Journal of Machine Tools and Manufacture*, 40:1141–1156, 2000.

[39] Y. S. Tarng, J. Y. Kao, and E. C. Lee. Chatter suppression in turning operations with a tuned vibration absorber. *International Journal of Materials Processing Technology*, 105:55–60, 2000.

[40] A. Preumont. *Vibration Control of Active Structures - An Introduction*. Kluwer Academic Publishers, 2002.

[41] D. K. Miu. Physical interpretation of transfer function zeros for simple control systems with mechanical flexibilities. *Journal of Dynamic Systems, Measurement and Control, Transactions of the ASME*, 113:419–423, 1991.

[42] D. Zimmerman and D. J. Inman. On the nature of the interaction between structures and proof-mass actuators. *AIAA Journal of Guidance*, 13:82–88, 1988.

[43] A. Cowley, A. Boyle. Active dampers for machine tools. *Annals of the CIRP*, 18:213–222, 1970.

[44] S. G. Tewani, K. E. Rouch, and B. L. Walcott. A study of cutting process stability of a boring bar with active dynamic absorber. *International Journal of Machine Tools and Manufacture*, 35(1):91–108, 1995.

[45] A. Harms, B. Denkena, and N. Lhermet. Tool adaptor for active vibration control in turning operations. In *Actuator, 2004*, pages 694–697, Bremen, Germany, 2004.

[46] N. Sims and Y. Zhang. Active damping for chatter reduction for high speed machining. *Proceedings of the AMAS workshop on smart materials and structures*, pages 195–212, 2003.

[47] Y. Zhang and N. Sims. Milling workpiece chatter avoidance uisng piezoelectric active damping: a feasibility study. *Smart Materials and Structures*, 14:N65–N70, 2005.

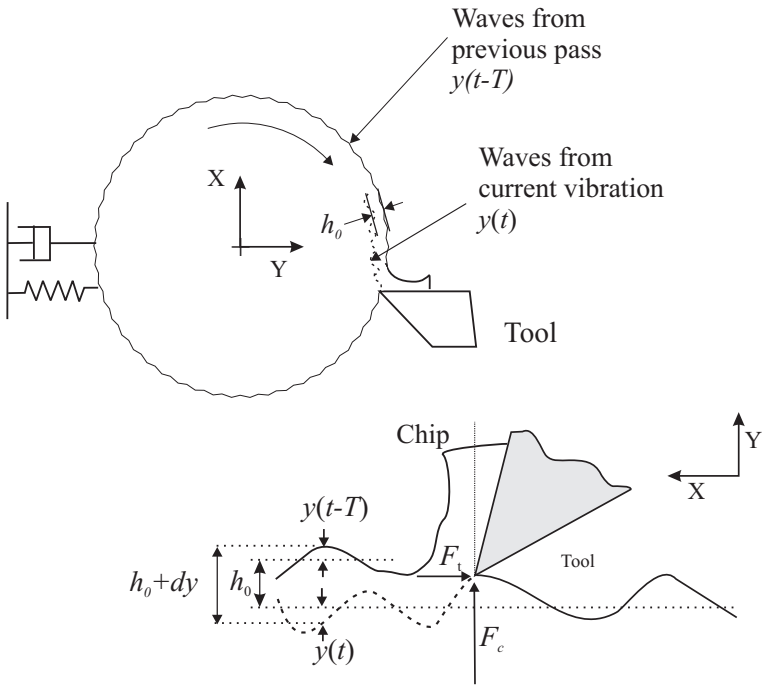

Figure 1: The regeneration process

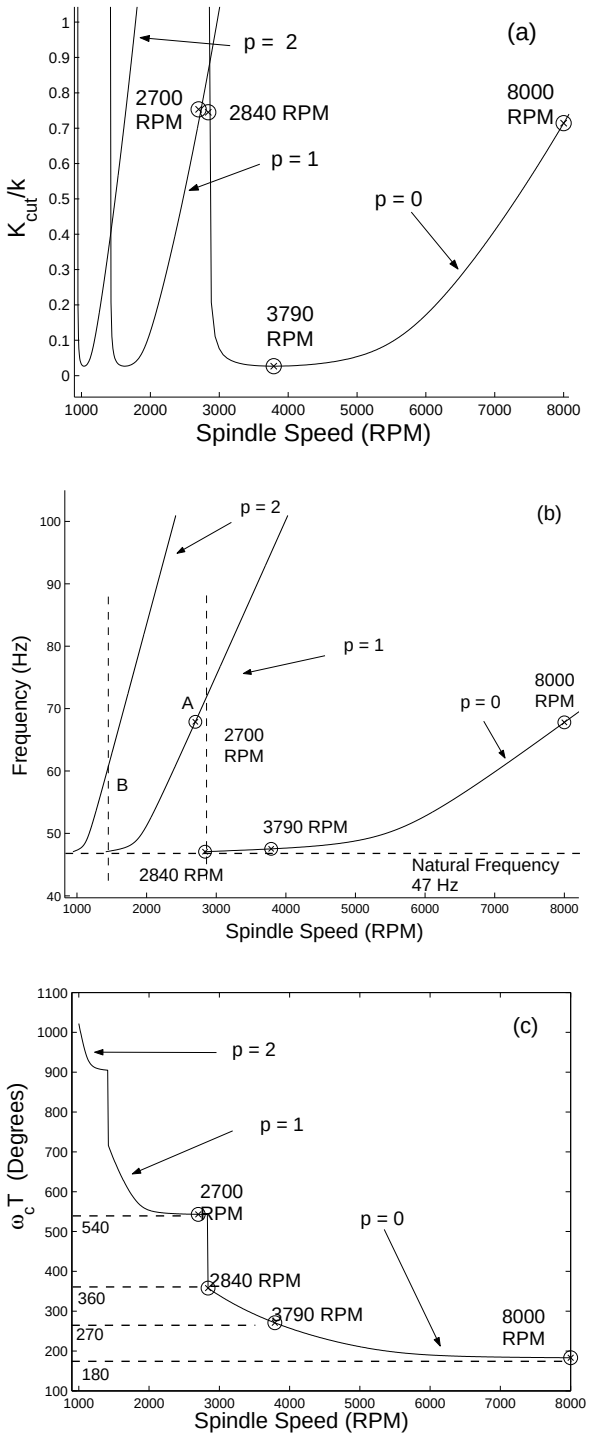

Figure 2: a)The stability lobe diagram b) Chatter frequencies c) Phase difference between successive undulations

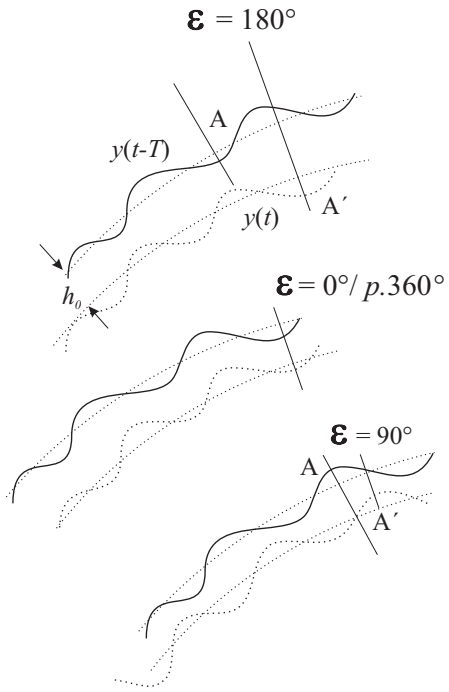

Figure 3: Phase difference between successive undulations on the workpiece surface

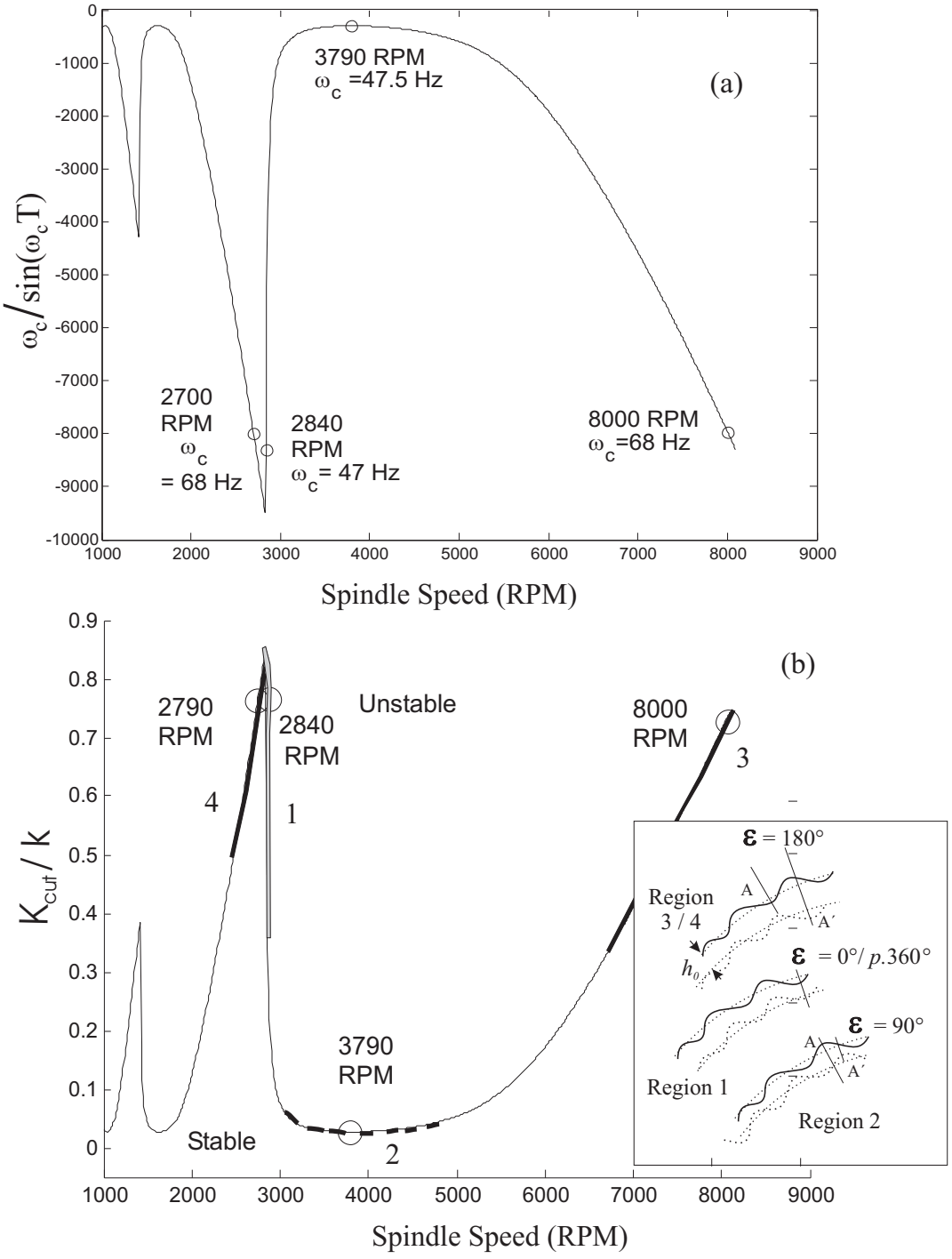

Figure 4: a)$\omega_c / \sin \omega_c T$ for various spindle speeds b)A typical stability lobe diagram

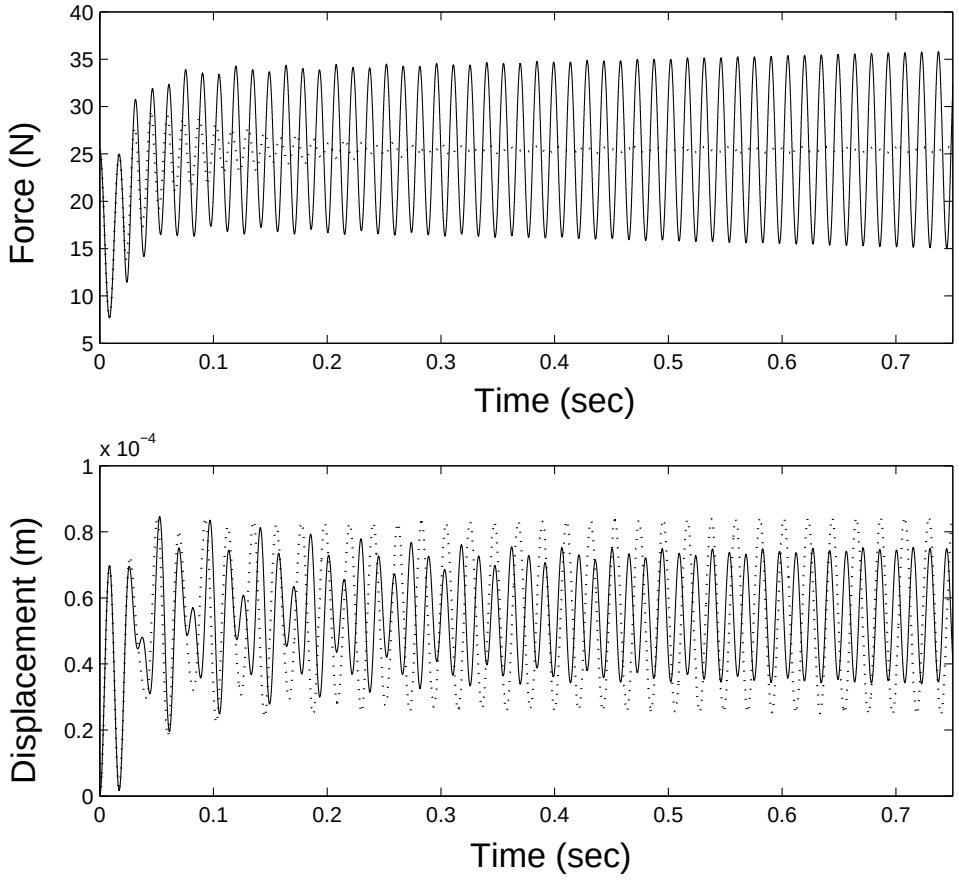

Figure 5: 2840 RPM (...): High stability due to constant excitation force, 2700 RPM (-): Highly dynamic excitation force and maximum stiffness causing low level of displacement

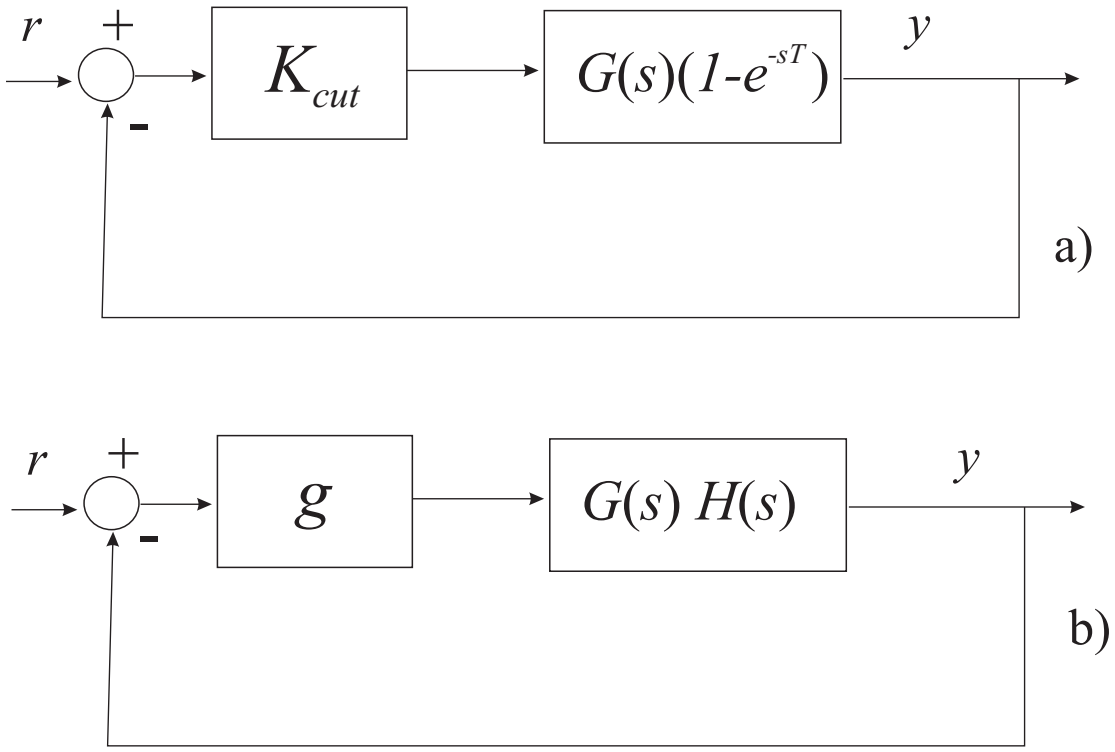

Figure 6: a)Chatter instability loop b) Classical closed loop system with unit feedback

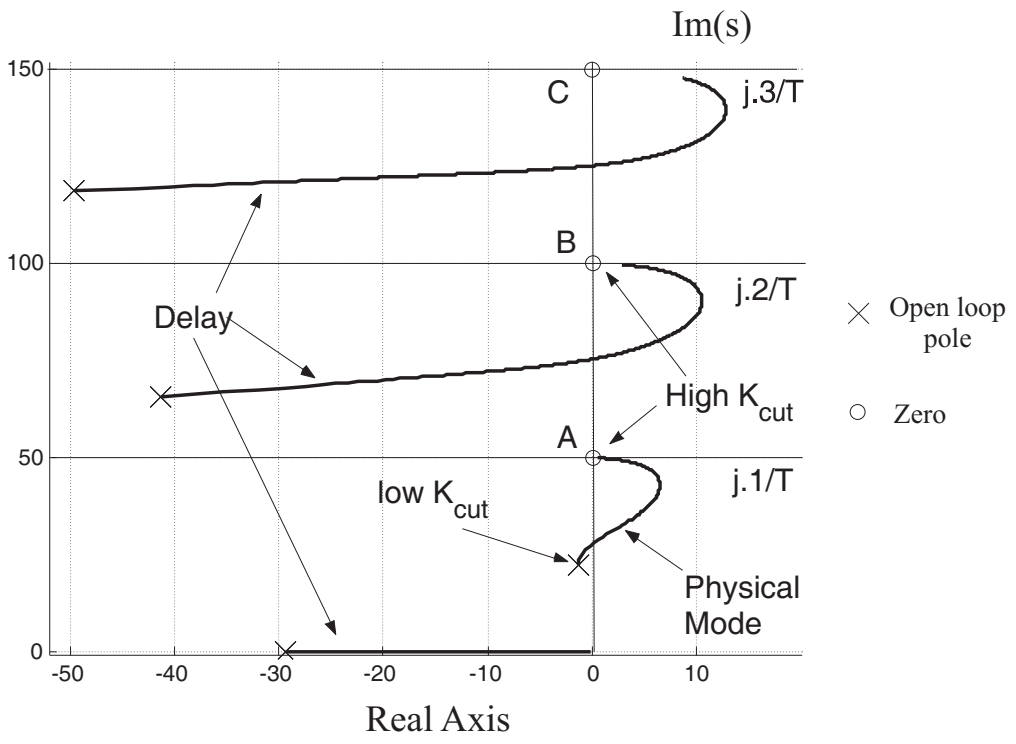

Figure 7: The locus of closed loop poles with increasing K_{cut}

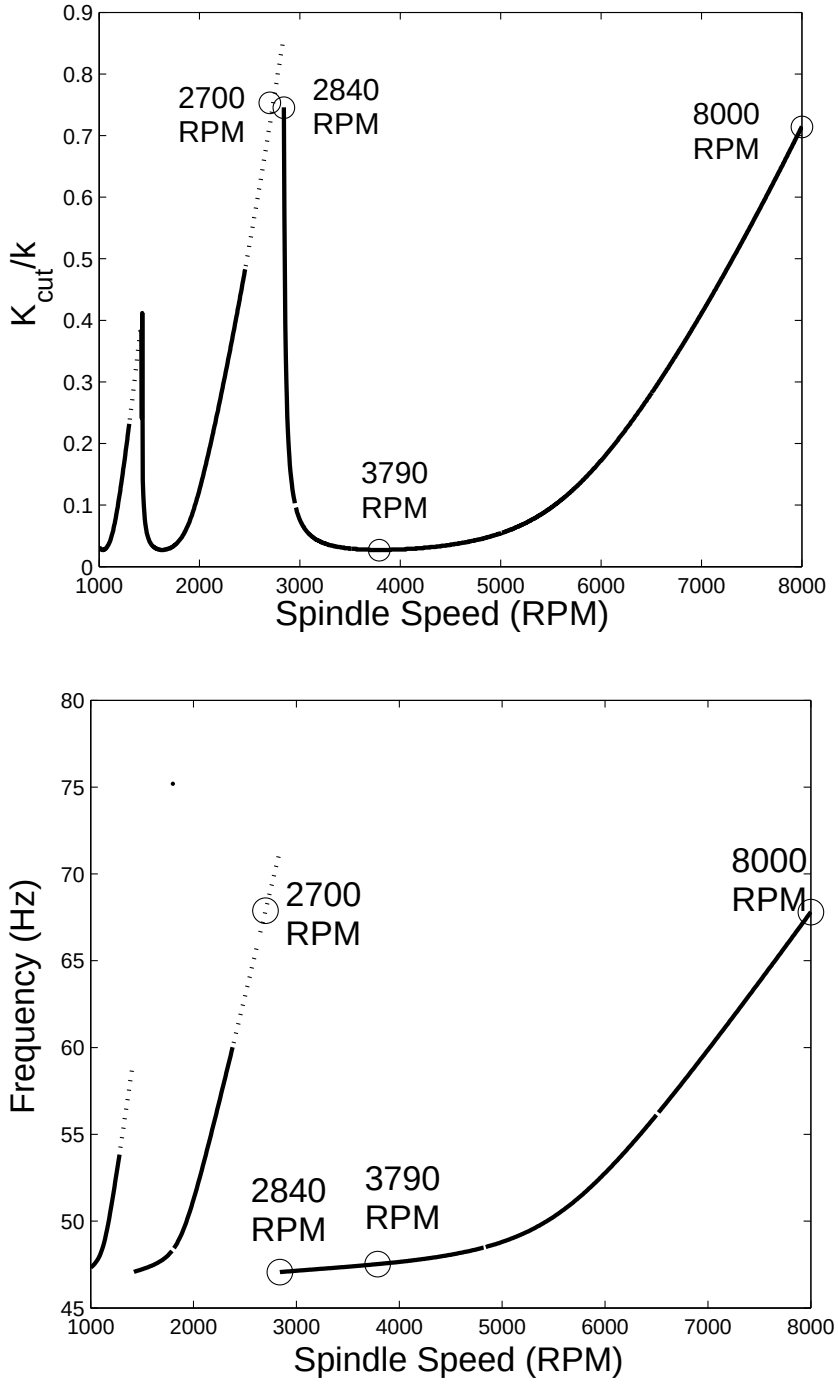

Figure 8: Stability lobe diagrams and chatter frequencies showing regions of instability arising from the structural mode (-) and the delay(...)

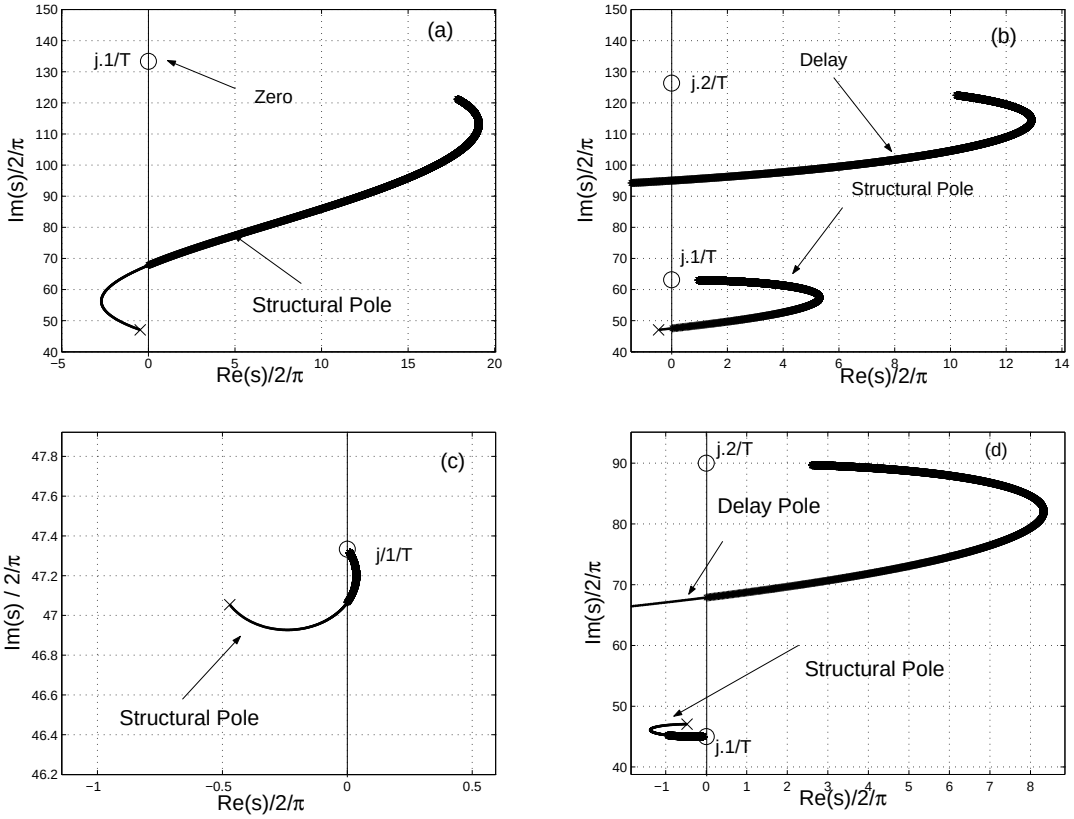

Figure 9: Loci of eigenvalues for a)8000 RPM b)3790 RPM c)2840 RPM d)2700 RPM

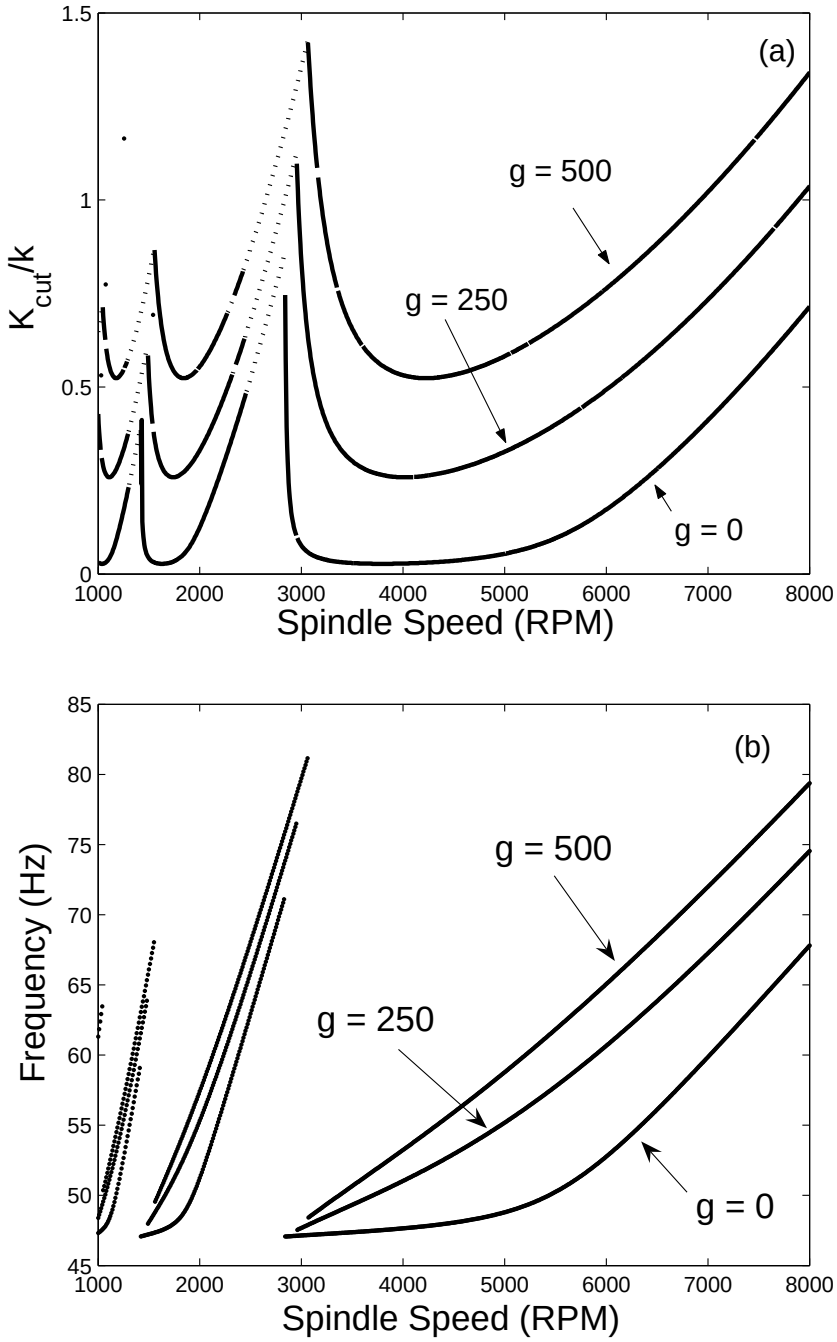

Figure 10: a) Comparison of stability lobes with and without active damping. Structural mode (-) Delay (...) b) Chatter frequencies with and without active damping

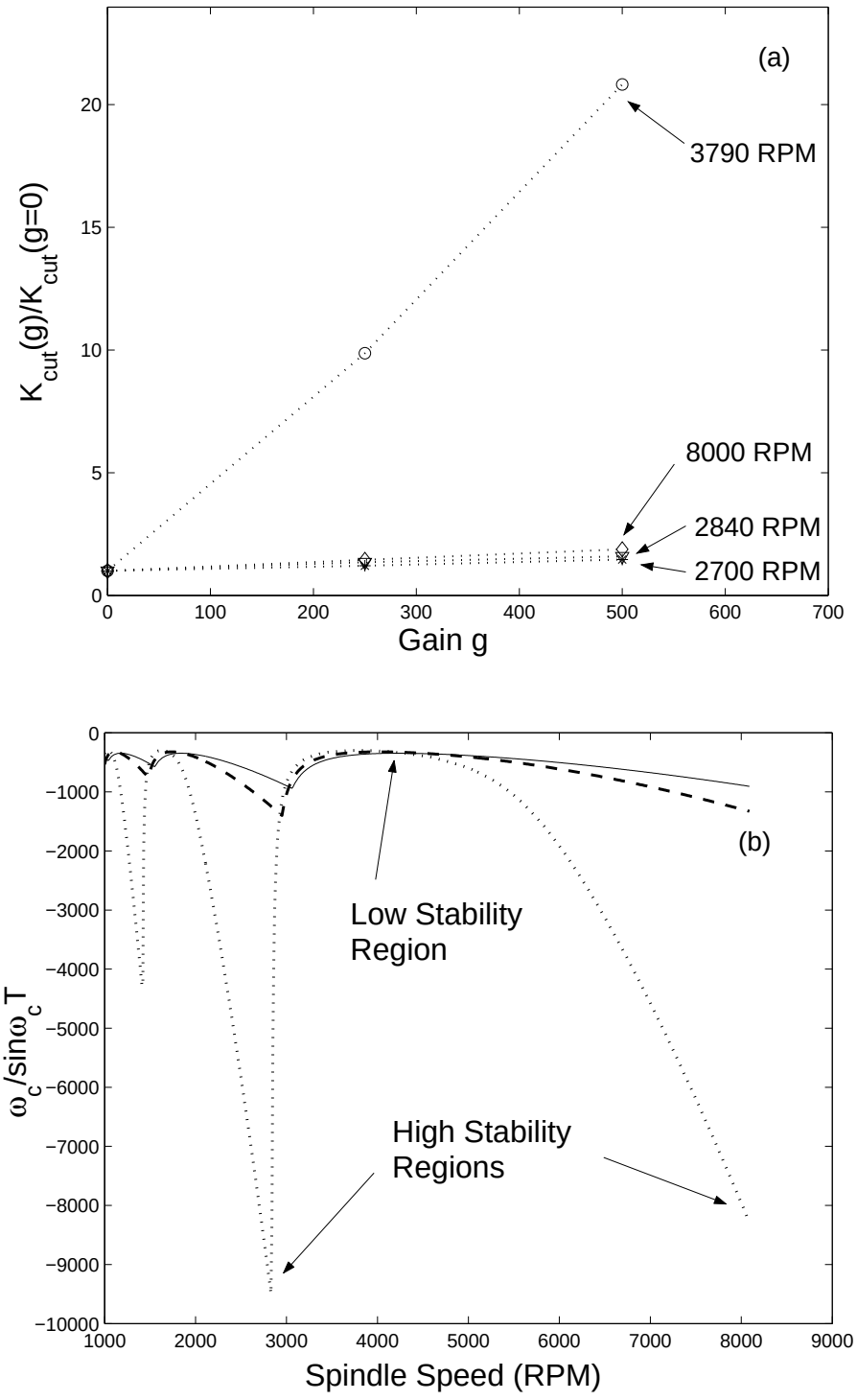

Figure 11: a) Ratio of stability limits with and without active damping for chosen spindle speeds b) Effect of active damping on $\omega_c/\sin\omega_c T$ for various spindle speeds; Gain values g=0 (...), g=250 (- - -), g=500 (-).

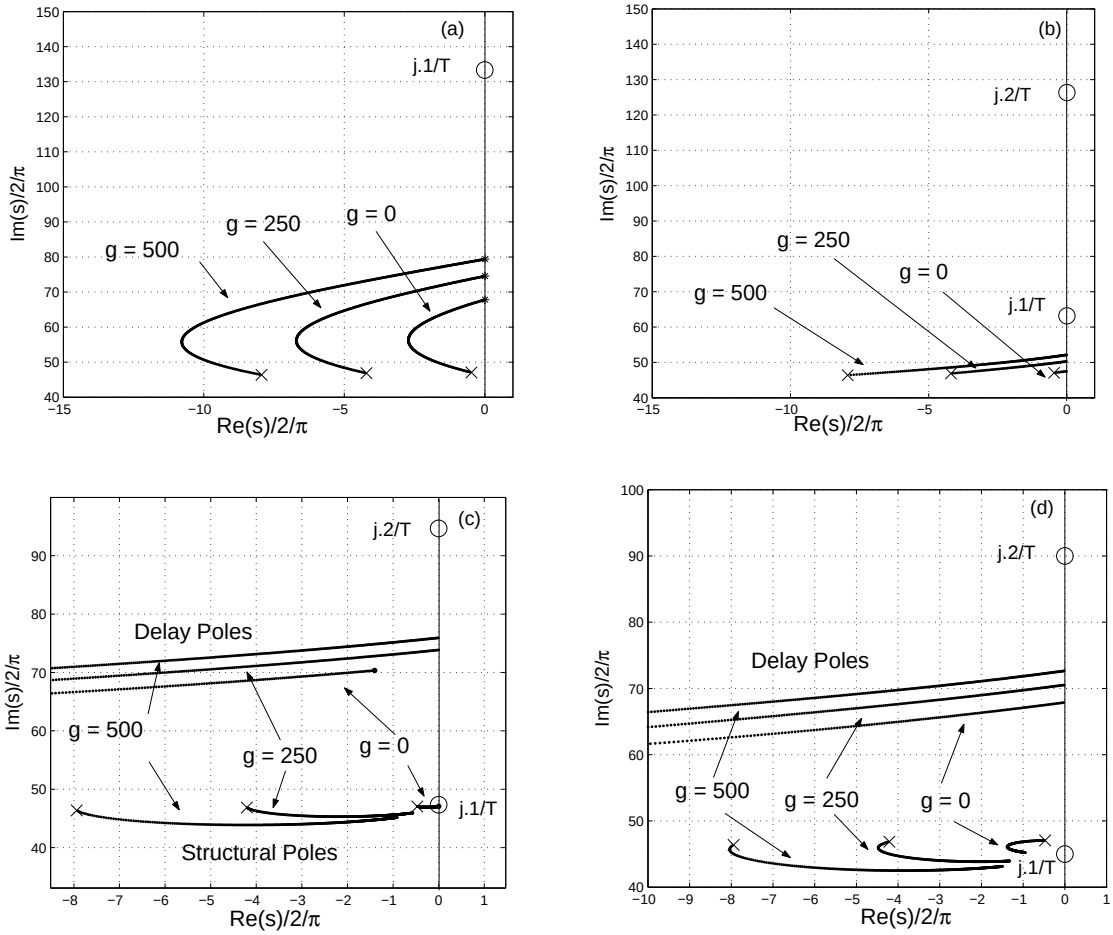

Figure 12: Effect of active damping for a) 8000 RPM b) 3790 RPM c) 2840 RPM d) 2700 RPM